Supplementary Information: Desalination and Hydrogen, Chlorine, and Sodium Hydroxide Production via Electrophoretic Ion Exchange and Precipitation

Viktor Shkolnikov, Supreet S. Bahga, Juan G. Santiago

Department of Mechanical Engineering, Stanford University, Stanford CA, USA

We here present additional information on the following topics:

SI 1. Composition of the sodium carbonate zone (trailing zone of anion exchange)

The ion concentration profiles for the anion exchange step are governed by electrophoretic migration, charge net neutrality of the zones, and the acid-base and precipitation reactions. During anion exchange, the leading, sodium chloride zone migrates towards the anode, followed by a growing, trailing zone of sodium carbonate (see Figure 1 of main text). The composition of the leading zone does not change during migration. Knowing the composition of the leading zone, we can calculate the composition of the trailing zone, using the electrophoretic migration equation integrated in space and time across the interface between the two zones. (We assume the composition of each zone is uniform.) This form of the electrophoretic migration equation can be written for sodium, chloride, and carbonic acid derivatives as

$$\left(c_{Na^+,NaCl} - c_{Na^+,Na^+/\overline{H_2CO_3}} \right) \frac{\Delta x}{\Delta t} = j \left(\frac{\mu_{Na^+,NaCl} c_{Na^+,NaCl}}{\sigma_{NaCl}} - \frac{\mu_{Na^+,Na^+/\overline{H_2CO_3}} c_{Na^+,Na^+/\overline{H_2CO_3}}}{\sigma_{Na^+/\overline{H_2CO_3}}} \right), \qquad (1)$$

$$\frac{\Delta x}{\Delta t} = j \left(\frac{\mu_{Cl^-,NaCl}}{\sigma_{NaCl}} \right), \qquad (2)$$

$$\frac{\Delta x}{\Delta t} = j\left(\frac{\mu_{\overline{H_2CO_3},Na^+/\overline{H_2CO_3}}}{\sigma_{Na^+/\overline{H_2CO_3}}}\right). \tag{3}$$

In our notation, the first subscript denotes the species of interest; the second subscript denotes the zone. Note we have assumed that chloride ions are not present in the sodium carbonate zone (trailing zone of anion exchange) and carbonic acid derivatives are not present in the sodium chloride zone (leading zone of anion exchange). Also, the overbar on the carbonic acid implies a summation of concentrations of all forms of carbonic acid derivatives. That is,

$$c_{\overline{H_2CO_3},Na^+/\overline{H_2CO_3}} = c_{CO_3^{2-},Na^+/\overline{H_2CO_3}} + c_{HCO_3^-,Na^+/\overline{H_2CO_3}} + c_{H_2CO_3,Na^+/\overline{H_2CO_3}}. \tag{4}$$

Similarly, the effective mobility[1] of carbonic acid derivatives $\mu_{\overline{H_2CO_3},Na^+/\overline{H_2CO_3}}$ is

$$\mu_{\overline{H_2CO_3},Na^+/\overline{H_2CO_3}} = \mu_{CO_3^{2-},Na^+/\overline{H_2CO_3}} \frac{c_{CO_3^{2-},Na^+/\overline{H_2CO_3}}}{c_{\overline{H_2CO_3},Na^+/\overline{H_2CO_3}}} + \mu_{HCO_3^-,Na^+/\overline{H_2CO_3}} \frac{c_{HCO_3^-,Na^+/\overline{H_2CO_3}}}{c_{\overline{H_2CO_3},Na^+/\overline{H_2CO_3}}}. \tag{5}$$

The conductivities of the sodium chloride, σ_{NaCl} and sodium carbonate $\sigma_{Na^+/\overline{H_2CO_3}}$ zones are

$$\sigma_{NaCl} = F\left(\left|\mu_{Na^+,NaCl}\right|c_{Na^+,NaCl} + \left|\mu_{Cl^-,NaCl}\right|c_{Cl^-,NaCl}\right), \tag{6}$$

$$\sigma_{Na^+/\overline{H_2CO_3}} = F\left(\left|\mu_{Na^+,Na^+/\overline{H_2CO_3}}\right|c_{Na^+,Na^+/\overline{H_2CO_3}} + 2\left|\mu_{CO_3^{2-},Na^+/\overline{H_2CO_3}}\right|c_{CO_3^{2-},Na^+/\overline{H_2CO_3}} + \left|\mu_{HCO_3^-,Na^+/\overline{H_2CO_3}}\right|c_{HCO_3^-,Na^+/\overline{H_2CO_3}}\right), \tag{7}$$

where F is Faraday's constant. The equations for local charge neutrality in the sodium chloride and sodium carbonate zones are, respectively,

$$c_{Na^+,NaCl} = c_{Cl^-,NaCl}, \tag{8}$$

$$c_{Na^+,Na^+/\overline{H_2CO_3}} = 2c_{CO_3^{2-},Na^+/\overline{H_2CO_3}} + c_{HCO_3^-,Na^+/\overline{H_2CO_3}}. \tag{9}$$

In equations (6) through (9), we neglect the contribution of hydrogen and hydroxyl ions to electroneutrality and zone conductivity. These assumptions have been termed "moderate pH" and "safe pH", respectively,[1] and are appropriate here as we expect hydrogen and hydroxyl ion concentrations to be significantly less than those of sodium, chloride or carbonic acid derivative ions. Lastly, we have equations for carbonic acid equilibrium:

$$K_{a1} = \frac{c_{H^+,Na^+/\overline{H_2CO_3}}c_{HCO_3^-,Na^+/\overline{H_2CO_3}}}{c_{H_2CO_3,Na^+/\overline{H_2CO_3}}}, \tag{10}$$

$$K_{a2} = \frac{c_{H^+,Na^+/\overline{H_2CO_3}}c_{CO_3^{2-},Na^+/\overline{H_2CO_3}}}{c_{HCO_3^-,Na^+/\overline{H_2CO_3}}}. \tag{11}$$

Here K_{a1} and K_{a2} are the dissociation constants for carbonic acid and bicarbonate, respectively. We solve equations (1) through (11) using an iterative solver described by Bahga et al.[2] To incorporate the dependence of electrophoretic mobility on ionic strength, the solver employs the

ionic strength correction module of SPRESSO.[3] We plot the concentration of sodium $c_{Na^+,Na^+/\overline{H_2CO_3}}$ and total concentration carbonic acid derivatives $c_{\overline{H_2CO_3},Na^+/\overline{H_2CO_3}}$ in the sodium carbonate zone in Figure S1 for feed water concentration of 100 to 600 mol m^{-3} sodium chloride.
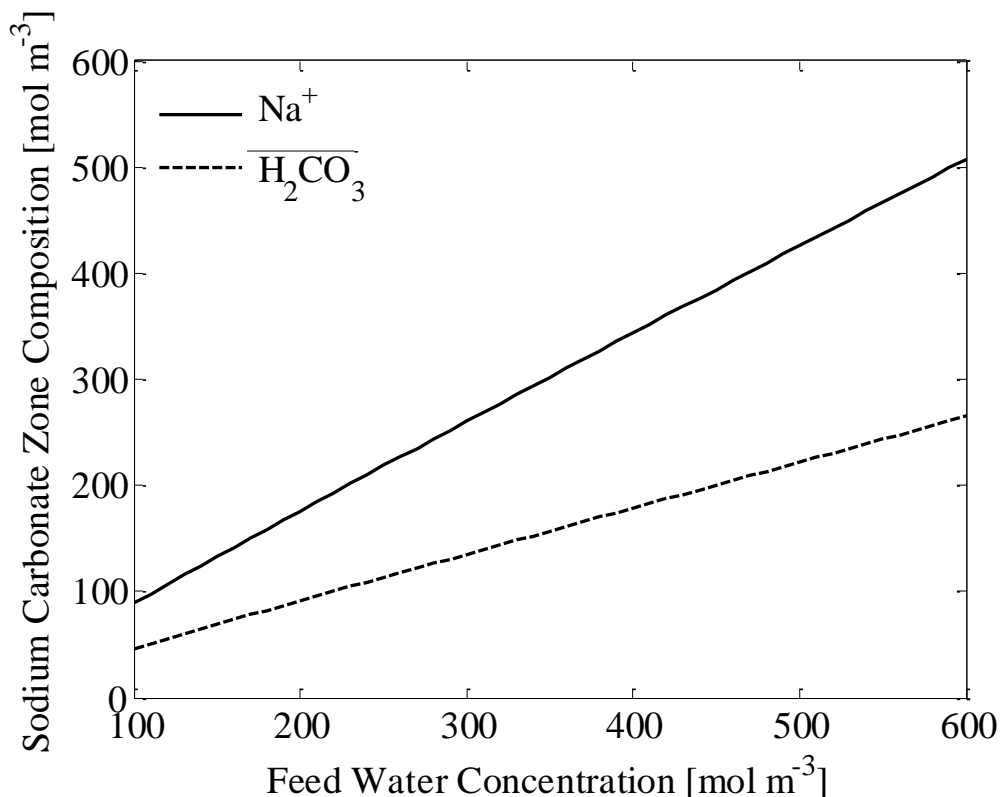
Figure S1. Theoretical concentration of sodium (solid line) and theoretical total concentration of carbonic acid derivatives (dashed line) as a function of feed water concentration in the sodium carbonate zone (trailing zone of anion exchange). We compute these using equation (2) of the main text for sodium, chloride, and carbonic acid ions together with the equations for carbonic acid equilibrium and local electroneutrality in each zone. In solving these, we neglect the contribution of hydrogen and hydroxyl ions to electroneutrality and zone resistivity. We expect the concentrations of hydrogen and hydroxyl ions to be significantly less than that of sodium, chloride or carbonic acid ions. To incorporate the dependence of electrophoretic mobility on ionic strength, we solve these equations with an in-house custom solver together with the electrophoresis simulator SPRESSO written in MATLAB.[4]

SI 2. Computing the composition and conductivity of the precipitate zone

To calculate the conductivity and the final composition of the precipitate zone we investigate two limiting cases: (1) precipitation reaction kinetics much slower than the electromigration rate, and (2) the precipitation kinetics much faster than the electromigration rate. We term "precipitation-to-migration timescale ratio" as the ratio of time scale to reach the precipitation reaction equilibrium and the electromigration time scale to enter the trailing zone.

In the case of the slow precipitation kinetics (large precipitation-to-migration time scale ratio), we assume the concentrations of calcium and carbonate in the trailing zone adjust to the concentration set by the leading zone, in accordance with current continuity and local electroneutrality in each zone. We also include in these calculations a carbonate content from the dissolved carbon dioxide originally in the water (due to equilibrium with the atmosphere). We then assume the precipitation reaction occurs as a subsequent process based on this initial condition.

In the case of fast precipitation kinetics (small precipitation-to-migration time scale ratio), the equilibrium concentrations of calcium and carbonate are dictated solely by the inlet and outlet conditions of a control volume analysis. The control volume is defined as the space occupied by the growing precipitate zone. This volume influxes and outfluxes calcium and carbonate (plus possess carbonate from the dissolved carbon dioxide originally in the water). In turn, these fluxes depend on the conductivity of the precipitate zone which we obtain from using the precipitation equilibrium equation. Thus, we solve iteratively the associated, coupled equations for influx, outflux, and precipitation equilibrium. Thus, this model assumes the species in the control volume are always at the equilibrium determined by precipitation and this equilibrium adjusts quickly to the influx or outflux of ions. We discuss in detail the formulation of each model below.

SI 2.1 Case of slow precipitation kinetics in cation exchange step

We define a control volume as the space containing the cation exchange trailing zone (precipitate zone). The calcium and carbonate species must obey the calcium and carbonate equilibrium relations:

$$c_{CO_2} = \frac{P_{CO_2}}{K_{Henry}}, \tag{12}$$

$$K_{a1} = \frac{c_{H^+} c_{HCO_3^-}}{c_{CO_2}}, \tag{13}$$

$$K_{a2} = \frac{c_{H^+} c_{CO_3^{2-}}}{c_{HCO_3^-}}, \tag{14}$$

$$K_{sp} = c_{Ca^{2+}} c_{CO_3^{2-}}, \tag{15}$$

$$K_w = c_{H^+} c_{OH^-}. \tag{16}$$

Here, K_{Henry} is Henry's constant for carbon dioxide, P_{CO2} is the partial pressure of carbon dioxide in the local atmosphere, K_w is the water dissociation constant, K_{sp} is the equilibrium dissociation constant for calcium carbonate, and K_{a1} and K_{a2} are the dissociation constants of carbonic acid. Equation (12) is Henry's law. Additionally, we expect net neutrality in the control volume:

$$c_{H^+} + 2c_{Ca^{2+}} = 2c_{CO_3^{2-}} + c_{HCO_3^-} + c_{OH^-}. \tag{17}$$

The control volume, grows with time from zero volume at $t = 0$. Thus all the calcium and carbonate accumulated in the control volume is equal to the respective, time-integrated influxes. This yields equations (4) and (5) of the main text, which we write here for convenience:

$$c_{Ca,EN} = c_{Ca^{2+}} + c_{CaCO_3(s)}, \tag{18}$$

$$c_{\overline{H_2CO_3},EN} = c_{CO_3^{2-}} + c_{HCO_3^-} + c_{CO_2} + c_{CaCO_3(s)} - c_{CO_2,OR}. \tag{19}$$

The subscripts EN and OR denote "entered" and "originally present". Following Deman,[5] we define $c_{CaCO_3(s)}$ as the moles of solid in the control volume divided by its entire volume. This is reasonable as we experimentally observed that the precipitate is fairly evenly dispersed in the control volume.

For slow precipitation equilibrium reactions, the concentrations of calcium and carbonate ions in the trailing zone adjust immediately to the conditions established by the leading zone, and only after that precipitation occurs. Under this assumption, the conservation of species and net neutrality yield:

$$c_{Ca,EN} = c_{Ca,adj}, \tag{20}$$

$$c_{\overline{H_2CO_3},EN} = c_{\overline{H_2CO_3},adj}, \tag{21}$$

where the subscript "adj" signifies the adjusted concentration (adjusted to the conditions established by the leading zone, see [6]). The adjusted concentrations are therefore calculated in the same manner as the adjusted (trailing zone) concentrations of the trailing zone of anion exchange. These concentrations are the total concentrations of all ionizations states of a chemical species. Lastly, the conductivity of the precipitate zone is:

$$\sigma_{ppt} = F\left(|\mu_{H^+}|c_{H^+} + |\mu_{OH^-}|c_{OH^-} + 2|\mu_{Ca^{2+},\infty}|c_{Ca^{2+}} + 2|\mu_{CO_3^{2-},\infty}|c_{CO_3^{2-}} + |\mu_{HCO_3^-,\infty}|c_{HCO_3^-}\right). \tag{22}$$

Here the subscript ∞ signifies that we take the mobility as that at infinite dilution. This is reasonable as we expect the concentration of calcium and carbonate to be low (less than 10 mM) and so the effect of ionic strength on mobility is expected to be small.[3] We simplify equations (12) through (22) into a single equation and solve iteratively using the bisection method.

SI 2.2 Case of fast precipitation kinetics in cation exchange step

We define the same control volume as in the previous section. The calcium and carbonate species then obey calcium and carbonate equilibrium relations (equations (12) through (16)), net electroneutrality (equation (17)) and calcium and carbonic acid flux conservation (equations (18) and (19)). The amount of calcium and carbonic acid which has entered the control volume (per volume of control volume) during the entire process is equal to the product of net flux (φ) in, channel cross-section area, A, and the total time for the process, t:

$$c_{Ca,EN} = \left(\varphi_{Ca,in} - \varphi_{Ca,out}\right)tA, \tag{23}$$

$$c_{\overline{H_2CO_3},EN} = \left(\varphi_{\overline{H_2CO_3},in} - \varphi_{\overline{H_2CO_3},out}\right)tA. \tag{24}$$

The time for the process is determined by the time for sodium to leave the channel. This can be expressed as follows:

$$t = \frac{c_{Na^+,Na^+/\overline{H_2CO_3}}}{A\varphi_{Na^+}}. \tag{25}$$

The flux of sodium is the sodium concentration multiplied by the electromigration velocity of sodium ions (which given by the mobility of sodium multiplied by the electric field). Employing Ohm's law ($E = j/\sigma$), we write this as:

$$\varphi_{Na^+} = \frac{jc_{Na^+,Na^+/\overline{H_2CO_3}}\mu_{Na^+,Na^+/\overline{H_2CO_3}}}{\sigma_{Na^+/\overline{H_2CO_3}}}. \tag{26}$$

The outflux of calcium is zero, as we assume a sharp boundary between the two zones. Similarly, the influx of calcium is given by:

$$\varphi_{Ca,in} = \frac{jc_{Ca^{2+}}\mu_{Ca^{2+},\infty}}{\sigma_{ppt}}. \tag{27}$$

The influx of carbonate ions (from the sodium carbonate zone) can be written as:

$$\varphi_{\overline{H_2CO_3},in} = \frac{jc_{\overline{H_2CO_3},Na^+/\overline{H_2CO_3}}\mu_{\overline{H_2CO_3},Na^+/\overline{H_2CO_3}}}{\sigma_{Na^+/\overline{H_2CO_3}}}, \tag{28}$$

where $c_{\overline{H_2CO_3},Na^+/\overline{H_2CO_3}}$ is the total concentration of all carbonic-acid-related species in the zone, and $\mu_{\overline{H_2CO_3},Na^+/\overline{H_2CO_3}}$ is their respective net mobility. $c_{\overline{H_2CO_3},Na^+/\overline{H_2CO_3}}$ is the concentration of the carbonic acid in the sodium carbonate zone after the anion exchange step (see SI 1). Lastly, we can write the flux of carbonate out of the control volume (into the anode reservoir) as:

$$\varphi_{\overline{H_2CO_3},out} = \frac{j\left(c_{CO_3^{2-}}\mu_{CO_3^{2-},\infty} + c_{HCO_3^-}\mu_{HCO_3^-,\infty}\right)}{\sigma_{ppt}}. \tag{29}$$

Putting together equations (23) through (29), we obtain that the concentrations of calcium and carbonate that entered the control volume as:

$$c_{Ca,EN} = \left(\frac{c_{Ca^+}\mu_{Ca^+,\infty}}{\sigma_{precipiate}}\right)\frac{\sigma_{Na^+/\overline{H_2CO_3}}}{\mu_{Na^+,Na^+/\overline{H_2CO_3}}}, \tag{30}$$

$$c_{\overline{H_2CO_3},EN} = \left(\frac{c_{\overline{H_2CO_3},Na^+/\overline{H_2CO_3}}\mu_{\overline{H_2CO_3},Na^+/\overline{H_2CO_3}}}{\sigma_{Na^+/\overline{H_2CO_3}}} - \frac{c_{CO_3^{2-}}\mu_{CO_3^{2-},\infty} + c_{HCO_3^-}\mu_{HCO_3^-,\infty}}{\sigma_{ppt}}\right)\frac{\sigma_{Na^+/\overline{H_2CO_3}}}{\mu_{Na^+,Na^+/\overline{H_2CO_3}}}. \tag{31}$$

Lastly, the conductivity of the precipitate zone is given by:

$$\sigma_{ppt} = F\left(\left|\mu_{H^+}\right| c_{H^+} + \left|\mu_{OH^-}\right| c_{OH^-} + 2\left|\mu_{Ca^{2+},\infty}\right| c_{Ca^{2+}} + 2\left|\mu_{CO_3^{2-},\infty}\right| c_{CO_3^{2-}} + \left|\mu_{HCO_3^-,\infty}\right| c_{HCO_3^-} \right). \quad (32)$$

To solve for the composition and conductivity of the precipitate zone, we simplify the equations above into a single equation and again solve iteratively using the bisection method.

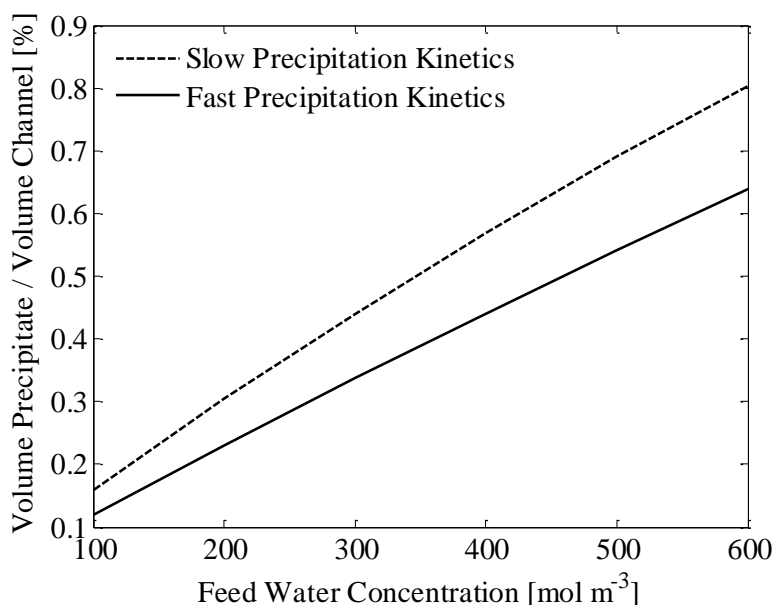### SI 3. Ratio of the precipitate volume to channel volume

In this section, we show that the volume of precipitate is negligible compared with the volume of the channel. We can estimate this from system-averaged molar density of the solid precipitate $c_{CaCO_3(s)}$ obtained in SI 2. We can write $c_{CaCO_3(s)}$ as:

$$c_{CaCO_3(s)} = \frac{N_{CaCO_3(s)}}{V_c}, \quad (33)$$

where, $N_{CaCO_3(s)}$ is the moles of calcium carbonate, and V_c is the volume of the channel. From this we write the ratio of precipitate volume to channel volume as:

$$\frac{V_{ppt}}{V_c} = c_{CaCO_3(s)} \frac{M_{CaCO_3(s)}}{\rho_{CaCO_3(s)}}, \quad (34)$$

where M is the molar mass and ρ is the density. Since we do not know the ratio of aragonite to calcite in the calcium carbonate precipitate that is formed in EPD, we assume that this ratio is 1:1 by volume and so take the density of the precipitate as 2750 kg m^{-3}.[7] We plot this in Figure S2.

Figure S2. Theoretical ratio of precipitate volume to channel volume as a function of feed water concentration (100 to 600 mol m^{-3} sodium chloride) based on the slow precipitation kinetics

(dashed line) and fast precipitation kinetics (solid line) models. Below a feed water concentration of 600 mol m^{-3} the precipitate occupies less than 1% of the channel volume and thus we neglect its volume in further analysis.

SI 4. Reagent consuption

Here we estimate the amount sodium carbonate and calcium chloride used per volume of channel and per volume of product water. The amount of sodium carbonate that is used, $N_{Na_2CO_3}$, is equal to the moles of carbonic acid derivatives which enter the channel in anion and cation exchange steps. The moles of carbonic acid derivative ions which enter the channel during anion exchange per volume of channel is the adjusted concentration of carbonic acid in the channel during the anion exchange. The moles of carbonic acid per volume of channel which enter the channel in the cation exchange is equal to the product of the flux of carbonic acid ($\varphi_{\overline{H_2CO_3},Na^+/\overline{H_2CO_3}}$), the channel cross-sectional area, and the time for cation exchange. We write the total amount as:

$$\frac{N_{Na_2CO_3}}{V_c} = c_{\overline{H_2CO_3},Na^+/\overline{H_2CO_3}} + \frac{\varphi_{\overline{H_2CO_3},Na^+/\overline{H_2CO_3}} A t_{catEx}}{V_c}. \tag{35}$$

The flux of carbonic acid ions in terms of the current density is

$$\varphi_{\overline{H_2CO_3},Na^+/\overline{H_2CO_3}} = \frac{jc_{\overline{H_2CO_3},Na^+/\overline{H_2CO_3}} \left|\mu_{\overline{H_2CO_3},Na^+/\overline{H_2CO_3}}\right|}{\sigma_{Na^+/\overline{H_2CO_3}}}. \tag{36}$$

The duration of the cation exchange step is equal to the time for sodium to leave the channel (see Figure 1, main text). The amount of sodium present in the channel at the start of cation exchange is the concentration of sodium in the sodium carbonate zone times the volume of the channel. The amount of sodium in the channel also equals the product of the flux of sodium out of the channel, the area of the channel, and the time for cation exchange. Thus the flux of sodium ions and the time for cation exchange is given by:

$$\varphi_{Na^+,Na^+/\overline{H_2CO_3}} = \frac{jc_{Na^+,Na^+/\overline{H_2CO_3}} \left|\mu_{Na^+,Na^+/\overline{H_2CO_3}}\right|}{\sigma_{Na^+/\overline{H_2CO_3}}}, \tag{37}$$

$$t_{catEx} = \frac{c_{Na^+,Na^+/\overline{H_2CO_3}} V_c}{\varphi_{Na^+,Na^+/\overline{H_2CO_3}} A} = \frac{V_c \sigma_{Na^+/\overline{H_2CO_3}}}{j\left|\mu_{Na^+,Na^+/\overline{H_2CO_3}}\right| A}. \tag{38}$$

Combining equations (35) and (36) with equation (38) we obtain the total consumption of sodium carbonate per volume of channel:

$$\frac{N_{Na_2CO_3}}{V_c} = c_{\overline{H_2CO_3},Na^+/\overline{H_2CO_3}} + \frac{c_{\overline{H_2CO_3},Na^+/\overline{H_2CO_3}} \left|\mu_{\overline{H_2CO_3},Na^+/\overline{H_2CO_3}}\right|}{\left|\mu_{Na^+,Na^+/\overline{H_2CO_3}}\right|}. \tag{39}$$

Since all of the channel and the calcium chloride reservoir gets filled with calcium carbonate precipitate, the moles of calcium consumed is the moles of carbonate consumed. We plot the consumption of calcium chloride and sodium carbonate per volume of channel in Figure S3a as a function of feed water concentration ranging 100 to 600 mol m^{-3} sodium chloride. In Figure S3b we plot also the consumption of calcium chloride and sodium carbonate per volume of product water. For the latter quantity, we divide equation (39) by the ratio of product water volume to channel volume. This ratio reflects the fact that some of desalinated water volume produced is used to create the calcium chloride and sodium carbonate solutions for the subsequent desalination cycle. We derive this ratio in Section SI 5.
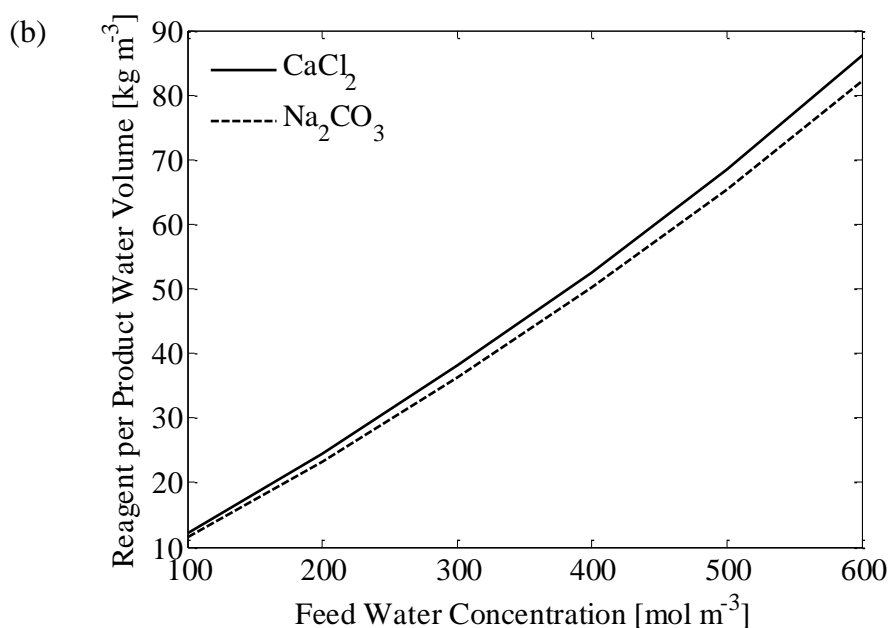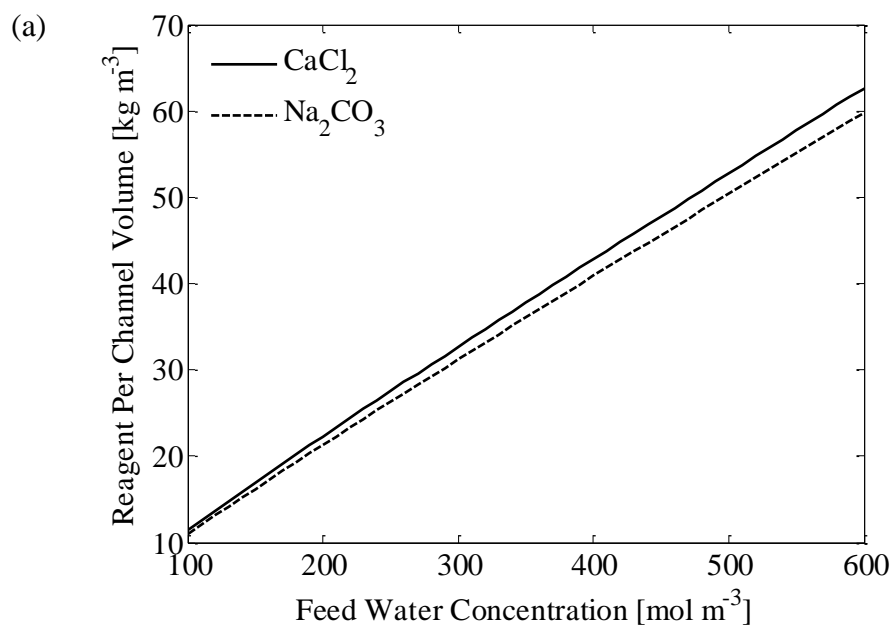
Figure S3. Calcium chloride (solid line) and sodium carbonate (dashed line) consumption as a function of feed water concentration (100 to 600 mol m^{-3} sodium chloride) per volume of channel (a) and per volume of product water (b). We obtain the reagent consumption per volume of product water by dividing reagent consumption per volume of channel by the ratio of product water volume to channel volume as a function of feed water concentration. This ratio is derived in Section SI 5.

SI 5. Permeate recovery ratio and product water to channel volume ratio

Permeate recovery ratio (*PRR*) is defined as product water flow rate per feed water flow rate.[8] Hence,

$$PRR = \frac{V_p}{V_f}, \tag{40}$$

where V_p and V_f are volumes of product water produced and feed water consumed, respectively. As we mention in the main text, one way to calculate *PRR* is to assume that calcium carbonate is recycled to aqueous calcium chloride and sodium carbonate (as we discuss in section 5.2 of the main text and in SI 12) and so no product water is consumed to produce the two reservoir solutions (and the net volume of product water produced would be the channel volume). However, to be conservative, we here estimate the net volume of product water as the volume of the channel minus the volumes of the sodium carbonate reservoir and the calcium chloride reservoir. This conservative estimate assumes that product water from an earlier desalination batch was used to make the necessary sodium carbonate and calcium chloride solutions from solid reagents. The volume of feed water consumed would then be the volume of the channel and that of the sodium chloride reservoir.

In a single run, we produce an amount of desalinated water equal to the volume of the channel. Since some of this water is used to fill the sodium carbonate and calcium carbonate reservoirs for the next run, the net water produced in a run is the volume of the channel minus the volumes of these reservoirs:

$$\frac{V_p}{V_c} = \frac{V_c - \left(V_{Na_2CO_3} + V_{CaCl_2}\right)}{V_c}. \tag{41}$$

The amount of feed water used is the volume of the channel plus the volume of the sodium chloride reservoir. Thus,

$$PRR = \frac{V_p}{V_f} = \frac{V_c - \left(V_{Na_2CO_3} + V_{CaCl_2}\right)}{V_c + V_{NaCl}}. \tag{42}$$

The volumes of the sodium carbonate and calcium chloride reservoirs are determined by the amount of these reagents used per run and the maximum solubility of these reagents. The maximum soluble concentrations for the reagents at room temperature are[7]

$$c_{Na_2CO_3,Max} = 2890 \text{ mol m}^{-3}, \tag{43}$$

$$c_{CaCl_2,Max} = 7300 \text{ mol m}^{-3}. \tag{44}$$

Thus, the above gives the volumes of the wells:

$$V_{Na_2CO_3} = \frac{\left(c_{\overline{H_2CO_3},Na^+/\overline{H_2CO_3}} + \frac{c_{\overline{H_2CO_3},Na^+/\overline{H_2CO_3}}\left|\mu_{\overline{H_2CO_3},Na^+/\overline{H_2CO_3}}\right|}{\left|\mu_{Na^+,Na^+/\overline{H_2CO_3}}\right|}\right)V_c}{c_{Na_2CO_3,Max}}, \tag{45}$$

$$V_{CaCl_2} = \frac{\left(c_{\overline{H_2CO_3},Na^+/\overline{H_2CO_3}} + \frac{c_{\overline{H_2CO_3},Na^+/\overline{H_2CO_3}}\left|\mu_{\overline{H_2CO_3},Na^+/\overline{H_2CO_3}}\right|}{\left|\mu_{Na^+,Na^+/\overline{H_2CO_3}}\right|}\right)V_c}{c_{CaCl_2,Max}}. \tag{46}$$

Substituting equations (45) and (46) into equation (41) yields the estimate net product water per volume of channel:

$$\frac{V_p}{V_c} = 1 - c_{\overline{H_2CO_3},Na^+/\overline{H_2CO_3}}\left(1 + \frac{\left|\mu_{\overline{H_2CO_3},Na^+/\overline{H_2CO_3}}\right|}{\left|\mu_{Na^+,Na^+/\overline{H_2CO_3}}\right|}\right)\left(\frac{1}{c_{Na_2CO_3,Max}} + \frac{1}{c_{CaCl_2,Max}}\right). \tag{47}$$

We use this ratio of product water volume to channel volume to obtain, for example, the reagent consumption per volume of product water in Section SI 4.

Next, we calculate the volume of the sodium chloride reservoir. Thus, we calculate the amount of required sodium chloride. The amount of sodium chloride needed in the sodium chloride reservoir is the product of the flux of sodium in the sodium chloride zone, the time of anion exchange, and the area of the channel:

$$\tag{48}$$

$$\frac{N_{NaCl}}{V_c} = \frac{\varphi_{Na^+,NaCl}At_{anEx}}{V_c}, \tag{49}$$

where the flux of sodium in the sodium chloride zone is given by:

$$\varphi_{Na^+,NaCl} = \frac{jc_{Na^+,NaCl}\left|\mu_{Na^+,NaCl}\right|}{\sigma_{NaCl}}. \tag{50}$$

The time for anion exchange is given by amount of chloride ions in the sodium chloride zone and their flux. The amount of chloride ions in the chloride zone per volume of channel is just the concentration of sodium chloride (the concentration of feed water):

$$c_{Cl^-,NaCl} = \frac{\varphi_{Cl^-,NaCl} A t_{anEx}}{V_c} = \frac{j c_{Cl^-,NaCl} \left| \mu_{Cl^-,NaCl} \right| A t_{anEx}}{\sigma_{NaCl} V_c}. \tag{51}$$

Thus, the time for anion exchange is given by:

$$t_{anEx} = \frac{\sigma_{NaCl} V_c}{j \left| \mu_{Cl^-,NaCl} \right| A}. \tag{52}$$

Combining equations (49), (50) and (52) we obtain the amount of sodium chloride required for the sodium chloride reservoir per volume of channel:

$$\frac{N_{NaCl}}{V_c} = \frac{c_{NaCl} \left| \mu_{Na^+,NaCl} \right|}{\left| \mu_{Cl^-,NaCl} \right|}. \tag{53}$$

The volume of the sodium chloride reservoir, V_{NaCl}, is then the amount of sodium chloride consumed divided by the feed water concentration, which simplifies (53) to

$$V_{NaCl} = \frac{\left| \mu_{Na^+,NaCl} \right|}{\left| \mu_{Cl^-,NaCl} \right|} V_c. \tag{54}$$

Combining this with equations (42), (45), and (46),

$$PRR = \frac{V_p}{V_f} = \frac{1 - c_{\overline{H_2CO_3},Na^+/\overline{H_2CO_3}} \left(1 + \frac{\left| \mu_{\overline{H_2CO_3},Na^+/\overline{H_2CO_3}} \right|}{\left| \mu_{Na^+,Na^+/\overline{H_2CO_3}} \right|}\right) \left(\frac{1}{c_{Na_2CO_3,Max}} + \frac{1}{c_{CaCl_2,Max}}\right)}{1 + \frac{\left| \mu_{Na^+,NaCl} \right|}{\left| \mu_{Cl^-,NaCl} \right|}}. \tag{55}$$

We plot the permeate recovery ratio as a function of feed water concentration in Figure S4.
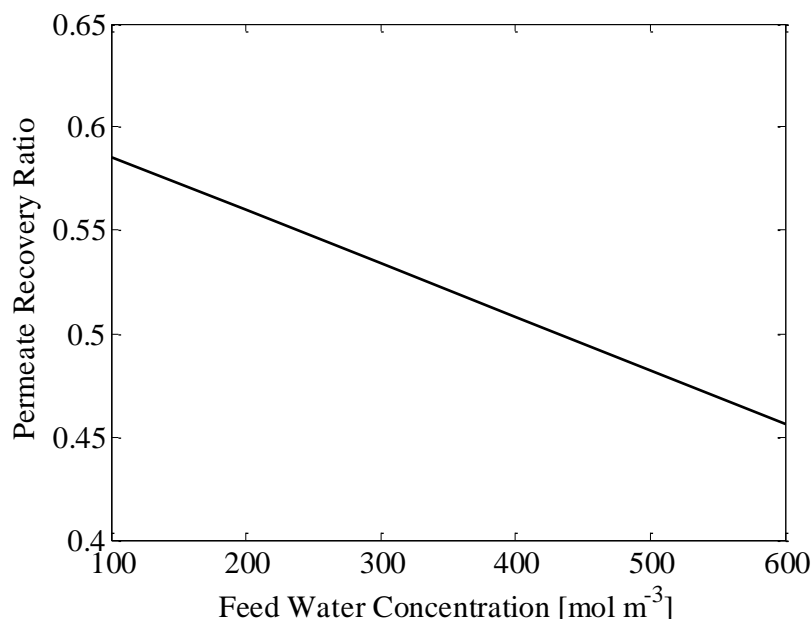
Figure S4. Permeate recovery ratio, *PRR*, as a function of feed water concentration. *PPR* varies approximately linearly from 58% to 46% as feed water concentration varies from 100 to 600 mol m^{-3} sodium chloride. In comparison, typical permeate recovery ratio for sea water reverse osmosis is around 30% to 50 %.[9]

SI 6. Energy consumption due to activation overpotentials

In this section, we show that the energy consumption due to activation overpotentials can be made negligible relative to energy consumption due to electrode reactions and ohmic looses. We anticipate low activation overpotentials, so we approximate them with the low activation over potential approximation to the Butler-Volmer equation[10] (valid for less than 15 mV at room temperature), given by

$$j = j_0 \frac{nF\eta_{act}}{RT},\tag{56}$$

where j is the current density based on electrode area, j_0 is the exchange current density, η_{act} is the activation overpotential, n is the number of electrons exchanged in the reaction, and R is the universal gas constant. For our anode and cathode reactions n is 2. Rearranging equation (56) to obtain the activation overpotential η_{act} in terms of current density in the channel ($j_{channel}$):

$$\eta_{act} = \frac{j}{j_0} \frac{RT}{nF} = \frac{1}{j_0} \frac{I}{A_{electrode}} \frac{RT}{nF} = \frac{1}{j_0} \frac{A_{channel}\, j_{channel}}{A_{electrode}} \frac{RT}{nF}.\tag{57}$$

Here $A_{channel}$ is the channel cross-sectional area and $A_{electrode}$ is the true electrode area. To minimize ohmic energy consumption, as described in Section 2.6.4 in the main text, we operate such that the width of the interface between the leading and trailing zone is 0.2 times the channel

length. This imposes a limit on the current density through the equations for interface width explained in Section 2.6.4 in the main text. We combine this limitation on current density, with equation (57) to obtain the activation over potential for the anion exchange:

$$\eta_{act,anEx} = \frac{5}{n}\frac{A_{channel}}{A_{electrode}}\left(\frac{RT}{F}\right)^2\frac{1}{H}\frac{\sigma_{NaCl}\mu_{\overline{H_2CO_3},Na^+/\overline{H_2CO_3}}}{\left(\mu_{Cl^-,NaCl} - \mu_{\overline{H_2CO_3},Na^+/\overline{H_2CO_3},}\right)}\left(\frac{1}{j_{0,H_2}} + \frac{1}{j_{0,Cl_2}}\right),\tag{58}$$

and for the cation exchange step,

$$\eta_{act,catEx} = \frac{5}{n}\frac{A_{channel}}{A_{electrode}}\left(\frac{RT}{F}\right)^2\frac{0.8\sigma_{ppt}}{H}\left(\frac{1}{j_{0,H_2}} + \frac{1}{j_{0,Cl_2}}\right).\tag{59}$$

To estimate the values of activation overpotentials, we use exchange current densities from O'Hayre et al. for the cathode (hydrogen generation) reaction[10] and from Anderson et al. for anode (chlorine generation) reaction[11] for smooth platinum electrodes. We also assume that device electrodes are rough, and conservatively assume that the true electrode area is 100 times greater than the smooth (geometric) area[12,13]. Thus, we obtain that for 300 mol m^{-3} sodium chloride feed water the activation overpotentials for anion and cation exchange are

$$\eta_{act,anEx} \approx \frac{A_{channel}}{A_{electrode}}\frac{0.00019\left[Vm\right]}{H},\tag{60}$$

$$\eta_{act,catEx} \approx \frac{A_{channel}}{A_{electrode}}\frac{2.5\times10^{-7}\left[Vm\right]}{H}.\tag{61}$$

Thus for channel length $H = 2$ cm, and $A_{channel}/A_{electrode}$ of unity, the activation overpotential for anion exchange would be around 9 mV and 0.01 mV for cation exchange for platinum electrodes. Similarly, for less expensive materials, for example nickel cathode and graphite anode, we estimate the activation overpotenials for anion exchange and cation exchange would be 90 mV and 0.2 mV respectively[14,15]. This is small compared to 2.19 V potential of electrode reactions (see Section 2.6.1 of main text), which comprise roughly 90% of the total energy consumption. The activation overpotentials can be made even smaller by decreasing channel cross-sectional area to electrode area or by increasing electrode roughness. Thus, we assume energy loss due to activation overpotentials can be made negligible for electrophoretic precipitative desalination.

SI 7. Amount of charge moved through the system in anion and cation exchange

The moles of negative charge transferred during the anion exchange per volume of channel is equal to the amount of chloride ions in the channel divided by the volume of the channel, i.e. the feed water concentration. Likewise, the moles of positive charge transferred during the cation exchange per volume of channel is equal to the difference in the sodium concentration between

the initial condition (feed water concentration) and the final condition (concentration of sodium in the sodium carbonate zone). Thus, the total moles of charge transferred during anion exchange, C_{anEx}, is given by

$$\frac{C_{anEx}}{V_c} = 2c_{NaCl} - c_{Na^+, Na^+/\overline{H_2CO_3}}. \tag{62}$$

The amount of charge passed in the cation exchange, C_{catEx}, is the amount of sodium migrated out of the channel plus the amount of carbonate migrated into the channel. Per volume of channel, this is equal to the concentration of sodium in the sodium carbonate zone plus the product of the flux of carbonic acid derivatives in the sodium carbonate zone, $\varphi_{\overline{H_2CO_3}, Na^+/\overline{H_2CO_3}}$, the channel cross-sectional area, time for cation exchange, and effective valence of the carbonic acid derivatives, $z_{\overline{H_2CO_3}, Na^+/\overline{H_2CO_3}}$, so

$$\frac{C_{catEx}}{V_c} = c_{Na^+, Na^+/\overline{H_2CO_3}} + \frac{\varphi_{\overline{H_2CO_3}, Na^+/\overline{H_2CO_3}} A t_{catEx} z_{\overline{H_2CO_3}, Na^+/\overline{H_2CO_3}}}{V_c}. \tag{63}$$

Combining equations (36), (38), and (63), we obtain

$$\frac{C_{catEx}}{V_c} = c_{Na^+, Na^+/\overline{H_2CO_3}} + c_{\overline{H_2CO_3}, Na^+/\overline{H_2CO_3}} \frac{\left|\mu_{\overline{H_2CO_3}, Na^+/\overline{H_2CO_3}}\right|}{\left|\mu_{Na^+, Na^+/\overline{H_2CO_3}}\right|}. \tag{64}$$

Combining equations (62) and (64), the total charge transferred during the whole process is

$$\frac{C_{total}}{V_c} = 2c_{NaCl} + c_{\overline{H_2CO_3}, Na^+/\overline{H_2CO_3}} \frac{\left|\mu_{\overline{H_2CO_3}, Na^+/\overline{H_2CO_3}}\right|}{\left|\mu_{Na^+, Na^+/\overline{H_2CO_3}}\right|}. \tag{65}$$

SI 8. Interface width between the sodium carbonate and precipitate zone

To obtain an expression for the interface width, we begin with the one-dimensional electromigration-diffusion equation:

$$\frac{\partial c_i}{\partial t} + \frac{\partial}{\partial x_1}\left(E\mu_i c_i - D_i \frac{\partial c_i}{\partial x_1}\right) = 0, \tag{66}$$

where x_1 is the coordinate along the length of the channel. We transform this equation into a coordinate system traveling with the interface, with the new length coordinate x. Thus, the electromigration-diffusion equation simplifies to

$$\frac{\partial}{\partial x}\left(E\mu_i c_i - D_i \frac{\partial c_i}{\partial x}\right) = 0, \tag{67}$$

which implies,

$$\left(E\mu_i c_i - D_i \frac{dc_i}{dx} \right) = const. \tag{68}$$

This constant is zero based the boundary conditions of constant concentrations of leading and trailing species as x tends to positive and negative infinity. Thus, at the interface, the electromigration flux balances the diffusion flux:

$$\mu_i c_i E = D_i \frac{dc_i}{dx}. \tag{69}$$

Substituting in a relation for Ohms's law into this flux balance results in:

$$\mu_i c_i \frac{j}{\sigma} = D_i \frac{dc_i}{dx}. \tag{70}$$

Next, we use a scaling argument and scale the interface length as dx, for concentration change across the interface dc. dx is the length over which dc occurs. To reflect the approximate scaling, we use Δc for dc and δ as the interface width:

$$\delta \approx \frac{D_i \sigma}{\mu_i c_i j} \Delta c_i. \tag{71}$$

To simplify, we use the Einstein- Smoluchowski relation for the diffusion constant, given by:

$$D_i = \frac{\mu_i k_B T}{z_i e}. \tag{72}$$

Employing the Einstein- Smoluchowski relation, we obtain a relation for the following diffusion length scale:

$$\delta \approx \frac{k_B T}{z_i e} \frac{\sigma}{j} \frac{\Delta c_i}{c_i}. \tag{73}$$

We define the interface width as the distance over which concentration changes from $0.9c_i$ to $0.1c_i$ and hence obtain

$$\delta \approx 0.8 \frac{k_B T}{z_i e} \frac{\sigma}{j}. \tag{74}$$

SI 9. Details of experimental protocol

As a laboratory demonstration to study process efficacy and to validate our model for energy consumption, we performed EPD on sodium chloride solutions in a microfluidic chip with four wells (Caliper Life Sciences, model NS12AZ). This miniature system also enabled excellent optical access to quantify ion densities and interface velocities. As we describe in the main text,

we first exchanged the anion, chloride, and then exchanged the cation, sodium. A typical experiment was initiated by filling west, north, and south well with sodium chloride solutions (see Figure S5, step 1). Next, we applied vacuum to the east well to fill all the channels in the chip with sodium chloride solution. The sodium chloride solution contained sodium chloride, 6-methoxy-N-(3-sulfopropyl)quinolinium (SPQ) anion visualization dye, and poly(vinylpyrrolidone) (PVP) (to suppress electroosmotic flow[16]). We then used vacuum to empty the east well and filled it with sodium carbonate solution. Next we placed platinum electrodes in the west (sodium chloride, anode) and east (sodium carbonate, cathode) wells and activated a constant current (Figure S5, step 2). We simultaneously recorded the applied voltages. We list the details of each solution composition and applied current density for each experiment in Table S1. Under applied electric field, the interface between the sodium chloride and the sodium carbonate zones migrates toward the anode. We observed the presence of a particular ion in a particular location of the chip by observing the fluorescence of SPQ in the region, as described in the main text.
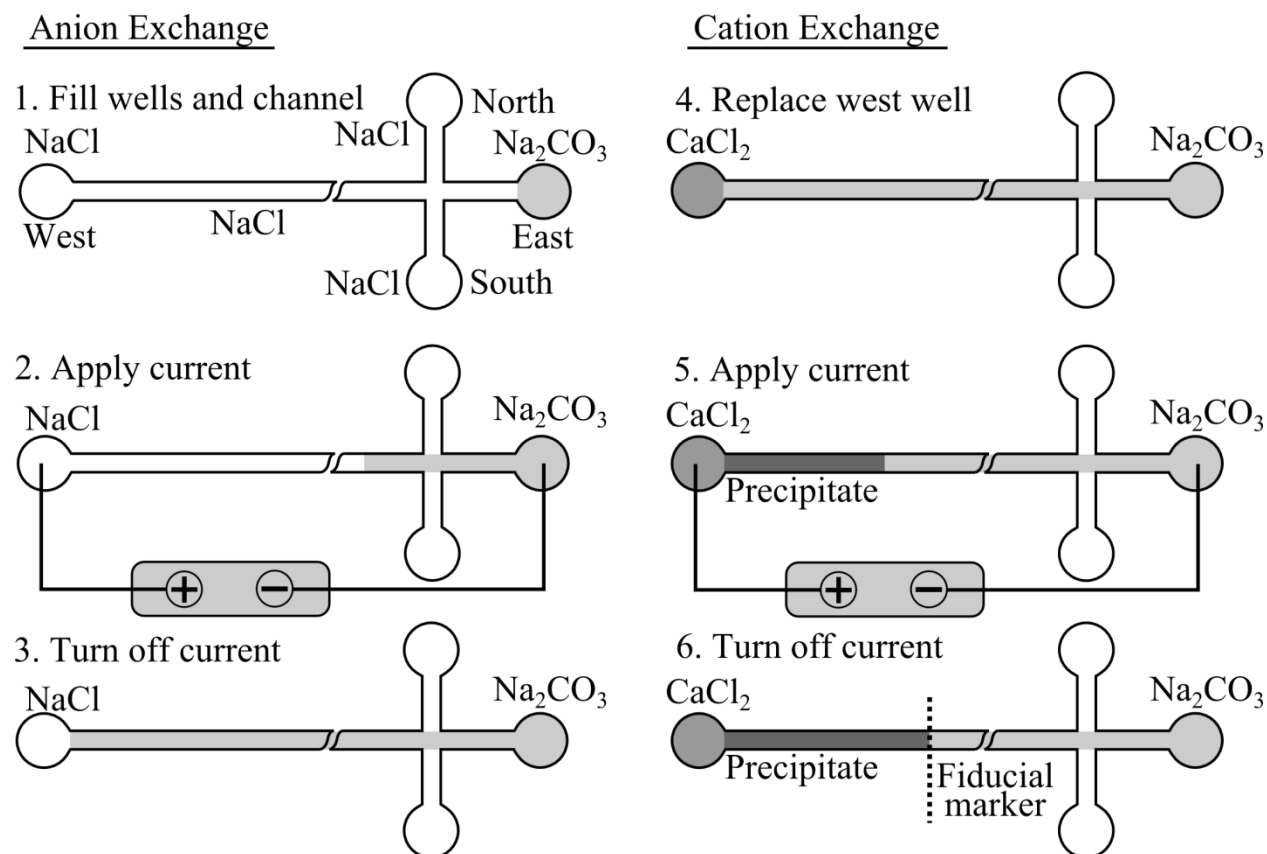
Figure S5. Schematic illustrating electrophoretic precipitate desalination process in a simple cross-pattern, glass microfluidic chip. 1. We first filled the north, south, and west wells with sodium chloride solutions, and applied vacuum to the east well to fill the channel. We then filled the east well with sodium carbonate solution. 2. We placed the anode into the sodium chloride well, and the cathode in the sodium carbonate well and applied an electric field. 3. Once the interface between the sodium chloride and sodium carbonate zones reached the west well, we

deactivated the current. 4. We vacuumed the west well and filled it with calcium chloride. 5. We placed the anode into the calcium chloride well, and the cathode in the sodium carbonate well and applied an electric field. 6. Once the interface between the precipitate zone and sodium carbonate interface reached a fiducial marker on the chip, we deactivated the current. We then cleaned the chip sequentially with hydrochloric acid, sodium hydroxide and deionized water to prepare the chip for the next experiment.

After the interface between the sodium chloride and sodium carbonate zones reached the west well we deactivated the current (Figure S5, step 3). We immediately emptied the west with vacuum, and fill the well with calcium chloride solution (Figure S5, step 4). We then placed the electrodes as before, and again applied a constant current, while measuring the associated voltages (Figure S5, step 5). At this point, under the influence of electric field, the calcium ions entered the channel, trailing the faster sodium ions. The calcium ions concurrently reacted with carbonate ions, which migrated towards the anode, to form calcium carbonate. Calcium carbonate precipitated out of solution, forming order 10 µm sized particles (see Figure 5c in the main text). We then let the precipitate interface migrate up to a fiducial marker in the channel and deactivated the current (Figure S5, step 6). We recorded white light illumination images of particles and fluorescence intensities of SPQ dye. In the precipitate zone the SPQ fluorescence intensity was high compared to the sodium carbonate zone (i.e. only weak quenching of SPQ). This indicated that carbonate concentration in the precipitate zone was much lower than in the calcium carbonate zone. In fact, the concentration of carbonate in the precipitate zone was below the resolution limit of SPQ. Thus, to infer the composition of the precipitate zone, we measured the conductivity of the precipitate zone. We describe how we estimated the precipitate zone conductivity and zone composition in SI 10.

After deactivating the current, we vacuum-emptied all the wells, filled the north, east, and south wells with deionized water and applied a vacuum to the west well. We then repeated this cleaning procedure with 1 M hydrochloric acid (to remove any remaining precipitate), 1 M sodium hydroxide (to neutralize the channel), and again with deionized water. Lastly, we rinsed all the wells with deionized water to prepare the chip for the next experiment.

Table S1
Summary of experimental conditions for data reported in Figures 2b, 3, and 5.

Reported in	Number of repeats	Composition of feed water solution	Composition of sodium carbonate solution	Composition of calcium chloride solution	Current density [a]
Figures 2b, 3	4	100 mM NaCl 1% (w/v) PVP 5.6 mM SPQ	100 mM Na_2CO_3 1% (w/v) PVP	100 mM $CaCl_2$ 1% (w/v) PVP	7.2 kA m^{-2} (0.72 kA m^{-2})
Figures 2b, 3	6	200 mM NaCl 1% (w/v) PVP 4 mM SPQ	200 mM Na_2CO_3 1% (w/v) PVP	200 mM $CaCl_2$ 1% (w/v) PVP	21 kA m^{-2} (2.1 kA m^{-2})
Figures 2b, 3	5	300 mM NaCl 1% (w/v) PVP 6.1 mM SPQ	300 mM Na_2CO_3 1% (w/v) PVP	300 mM $CaCl_2$ 1% (w/v) PVP	12 kA m^{-2} (1.2 kA m^{-2})
Figures 2b, 3	7	400 mM NaCl 1% (w/v) PVP 4 mM SPQ	400 mM Na_2CO_3 1% (w/v) PVP	400 mM $CaCl_2$ 1% (w/v) PVP	43 kA m^{-2} (1.6 kA m^{-2})
Figures 2b, 3	6	500 mM NaCl 1% (w/v) PVP 4 mM SPQ	500 mM Na_2CO_3 1% (w/v) PVP	500 mM $CaCl_2$ 1% (w/v) PVP	53 kA m^{-2} (1.6 kA m^{-2})
Figures 2b, 3	6	600 mM NaCl 1% (w/v) PVP 5.4 mM SPQ	600 mM Na_2CO_3 1% (w/v) PVP	600 mM $CaCl_2$ 1% (w/v) PVP	24 kA m^{-2} (2.4 kA m^{-2})
Figures, 5a, 5b	1	300 mM NaCl 1% (w/v) PVP 6.1 mM SPQ	300 mM Na_2CO_3 1% (w/v) PVP	300 mM $CaCl_2$ 1% (w/v) PVP	3.3 kA m^{-2} (3.3 kA m^{-2})
Figure 5c	1	200 mM NaCl 1% (w/v) PVP 6.1 mM SPQ	200 mM Na_2CO_3 1% (w/v) PVP	200 mM $CaCl_2$ 1% (w/v) PVP	3.3 kA m^{-2} (0.96 kA m^{-2})

[a] Current density for anion exchange and in parenthesis for cation exchange.

SI 10. Experimentally estimating the conductivity and composition of the precipitate zone

We obtained the conductivity of the precipitate zone from the measured total resistance of the channel. During cation exchange, we measured set current and measured voltage, and thus obtained the channel resistance, R, as a function of time. R is related to interface position x by

$$R = \frac{x}{\sigma_T A} + \frac{H - x}{\sigma_L A}, \tag{75}$$

where H and A are channel length and channel cross sectional area, respectively. σ_L and σ_T are the conductivities of the leading and trailing zone respectively. Employing equation (3) in the main text for interface velocity, we can write the channel resistance as a function of time t as

$$R = \frac{I\mu_{i,L}}{A^2}\left(\frac{1}{\sigma_T\sigma_L} - \frac{1}{\sigma_L^2}\right)t + \frac{H}{\sigma_L A},\tag{76}$$

where $\mu_{i,L}$ is the mobility of the leading ion in the leading zone. We rearrange this to obtain the conductivity of the trailing zone σ_T as a function of time, current density j, and instantaneous applied voltage V as

$$\sigma_T = \left[\frac{1}{j\mu_{i,L}}\left(\frac{V}{t}\sigma_L - \frac{H}{At}\right) + \frac{1}{\sigma_L}\right]^{-1}.\tag{77}$$

We fit the measured instantaneous applied voltage V *versus* time to equation (77) to obtain σ_T, the conductivity of the precipitate zone. After obtaining the conductivity, we estimated the composition of the precipitate zone, by solving precipitate zone composition equations described in section SI 2.

SI 11. SPQ quenching constants for chloride and carbonate anions

We obtained the quenching constants by fitting the Stern-Volmer equation (equation (17) in Section 3.3 of the main text) with SPQ florescence intensity at seven concentrations of the quenching ion ranging from 0.05 M to 0.35 M and SPQ fluorescence intensity in the absence of quencher. For this calibration, we prepared separate solutions of sodium chloride and sodium carbonate (both obtained from Sigma-Aldrich, St. Louis, MO) from 0.05 to 0.35 M with 0.004 M 6-methoxy-N-(3-sulfopropyl)quinolinium (SPQ) (from Invitrogen, Carlsbad, CA) in deionized ultrafiltered water from Fischer Scientific (Pittsburgh, PA). We then measured the fluorescence of each solution and a standard 0.004 M SPQ solution, using a NanoDrop 3300 Fluorospectrometer (Thermo Scientific, Wilmington, DE). Fitting the fluorescence of each solution using the Stern-Volmer equation, we obtained quenching constants for chloride and carbonate to be 107 M^{-1} and 25 M^{-1} respectively. We note that the fluorescence quenching appears to obey the Stern-Volmer equation between 0.05 and 0.35 M for sodium chloride and sodium carbonate.
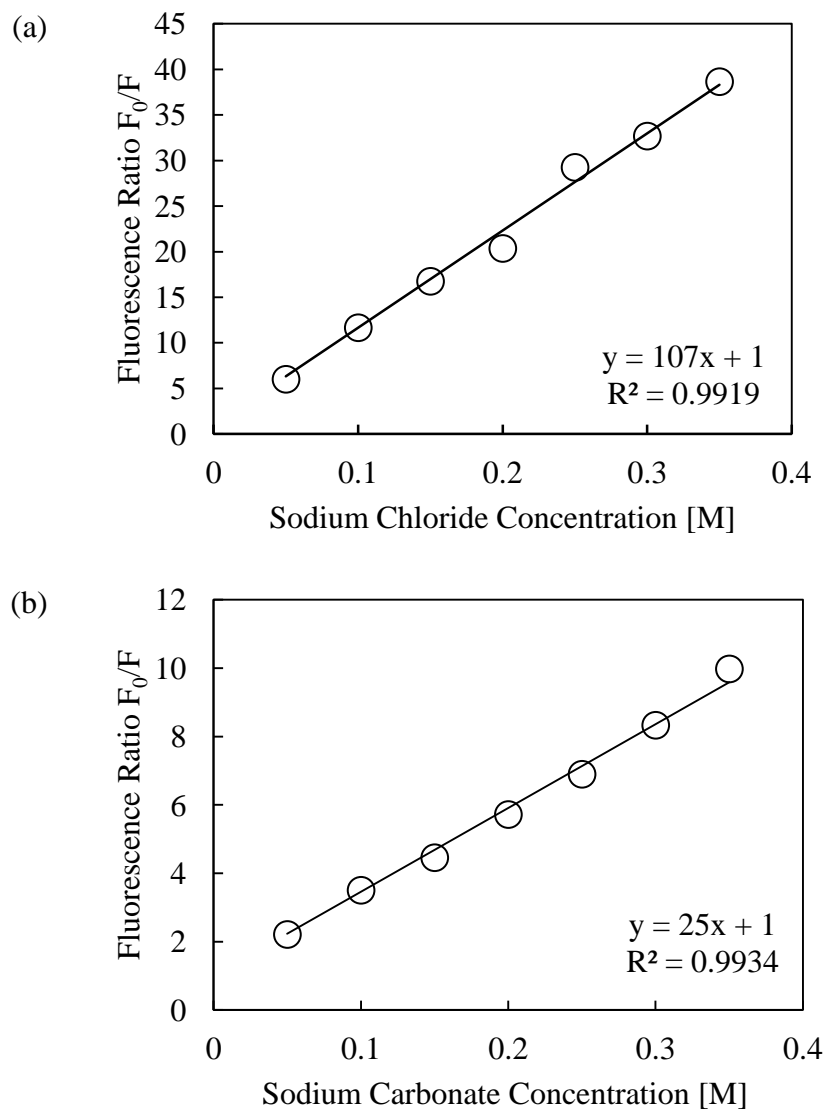
Figure S5. Fluorescence ratio as a function of concentration of sodium chloride (a) and sodium carbonate (b). The slope of the fitted linear curve indicates the quenching constant for each species as per the Stern-Volmer Equation. The regression coefficients R^2 for both sodium chloride (a) and sodium carbonate (b) data were above 0.99, indicating a good fit of the experimental data to the Stern-Volmer Equation. The quenching constants for chloride and carbonate were 107 M^{-1} and 25 M^{-1} respectively.

SI 12. Reagent recycling using the Solvay process

We hypothesize that for the calcium carbonate EPD system that we describe in the main text, sodium carbonate and calcium chloride can be regenerated using a modified Solvay process. Solvay process is discussed in detail in [17]. In the modified Solvay process, calcium carbonate is first heated to produce calcium oxide and carbon dioxide:

$$CaCO_3 \rightarrow CaO + CO_{2(g)}. \tag{78}$$

The carbon dioxide is then reacted with brine and ammonia to produce sodium bicarbonate and ammonium chloride:

$$NaCl + NH_3 + CO_2 \rightarrow NaHCO_3 + NH_4Cl. \tag{79}$$

Sodium bicarbonate is then heated to produce sodium carbonate, water, and carbon dioxide:

$$2NaHCO_3 \rightarrow NaCO_3 + H_2O + CO_{2(g)}. \tag{80}$$

At this point, the resulting solution can be used in the anion exchange step of EPD. To generate calcium chloride, calcium oxide from (78) is reacted with water and ammonium chloride from (79). This yields calcium chloride, water, and ammonium, which is reused in step (79):

$$CaO + H_2O + 2NH_4Cl \rightarrow CaCl_2 + 2NH_3 + 2H_2O. \tag{81}$$

The net process consumes 2 moles of sodium chloride and produces 1 mole sodium carbonate and 1 mole of calcium carbonate as well as 2 moles of water per mole of calcium carbonate. The process is net exothermic and produces 550 kJ per mole of calcium carbonate.

SI 13: Method scale-up with multiple channels in parallel

In Figure S6 we show a schematic demonstrating one simple scale-up concept for EPD; using multiple channels in parallel. Many parallel channels can share a single, large anodic reservoir and a single large cathodic reservoir (with a single pair of electrodes).
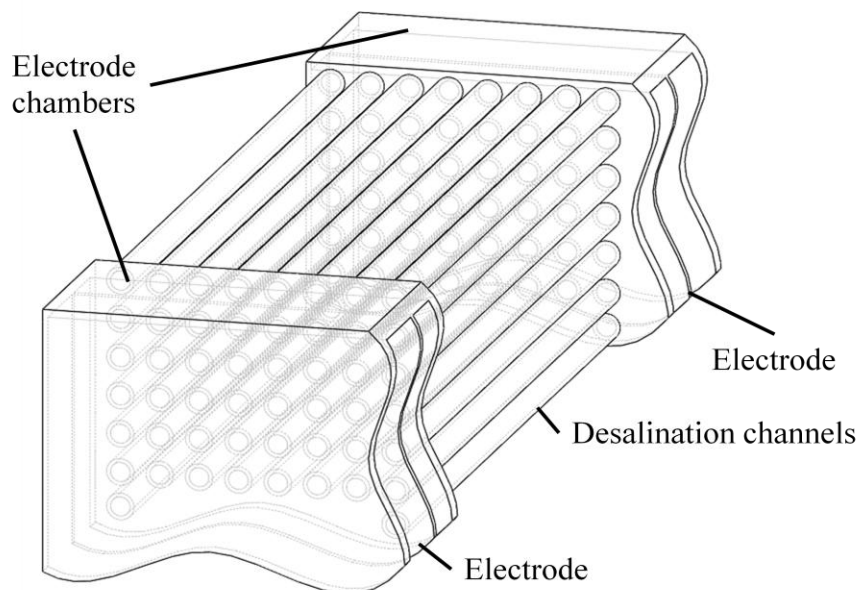
Figure S6. Cutaway schematic demonstrating a potential scale-up concept for EPD using multiple channels in parallel. The anodic and cathodic electrode chambers are connected by many desalination channels in parallel. A single pair of electrodes serves the entire device.

SI 14:   Scale-up concept using continuous free flow process

We envision that EPD may be scaled-up as a continuous flow process (see Figure SI 7). In a continuous flow process the leading zone (feed water zone in anion exchange and sodium carbonate zone in cation exchange) starts out flowing between electrode structures, while well solutions flow on the other side of electrode structures. A constant potential is applied between the electrode structures, causing shockwaves described in the main text to propagate in the *y*-direction, and trialing zones to develop.

In this section we present a rough estimate of the ohmic energy consumption and energy consumption due to pumping in a free flow process. The ohmic energy consumption in a free flow process scales similarly as that in a batch process described in the main text. As we shall describe, the energy consumption due to pumping in a typical free flow setup is negligible compared to other forms of energy consumption.

14.1 Ohmic energy consumption in a continuous free flow process
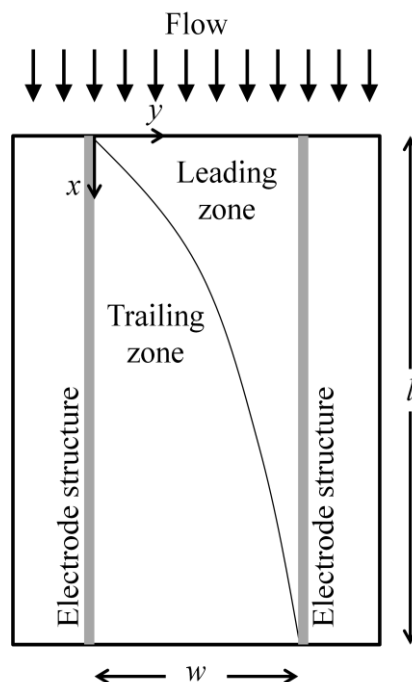
Figure S7. Schematic of free flow concept for EPD. The leading zone (feed water zone in anion exchange and sodium carbonate zone in cation exchange) flows between electrode structures, while reagent solutions flow on the other side of porous electrode structures. The flow in the x-direction is driven by pressure. A constant potential is applied between the electrode structures, causing shockwaves described in the main text to propagate in the y-direction, and trialing zones to develop.

Here we analyze a continuous free flow cell (see Figure SI 7) that is a vertical prism of height h, length l, and width w. We follow an analysis similar to that of Kasicka et $al.$[18] In this cell, the hydrodynamic flow is in the x direction, while the electric field is applied perpendicular to the flow, in the y direction. Following Kasicka et $al.$ we assume the hydrodynamic flow is uniform across y and z coordinates and is strictly in the x direction with velocity u_x. A charged species in this flow attains a velocity u_x in the x direction and electrophoretic drift velocity u_y in the y-direction when electric field is applied. The electrophoretic velocity is given by $u_y = \mu_L E_L$ where E_L is the electric field in the leading zone (see Section 2.3 in the main text). Note that $u_x = dx/dt$ and $u_y = dy/dt$. Thus

$$u_y/u_x = dy/dx. \tag{82}$$

This equation will form the basis of the differential equation describing the interface between the leading and trailing zones.

We consider an infinitesimal segment of the prism with dimensions $dx \cdot w \cdot h$. For this segment the total width w, total voltage V, and total resistance of the segment dR is

$$w = d_T + d_L, \tag{83}$$

$$V = V_T + V_L, \tag{84}$$

$$dR = dR_T + dR_L, \tag{85}$$

where the subscripts T and L indicate trailing zone and leading zone respectively. Note that the location of the interface, y, is given by

$$y = d_T = w - d_L. \tag{86}$$

Using (86) and definition of resistance we can write (85) as

$$dR = \left(\frac{1}{hdx} \right) \left(\frac{y}{\sigma_T} + \frac{w-y}{\sigma_L} \right), \tag{87}$$

and electrophoretic velocity as

$$u_y = \mu_L \frac{V_L}{w - y}. \tag{88}$$

Next, using Ohm's law, the voltage across the leading zone in this segment is

$$V_L = V \frac{dR_L}{dR}. \tag{89}$$

Combining equations (82) and (87) through (89) we obtain a differential equation for the curve describing the interface between the leading and trailing zones

$$\frac{dy}{dx} = \frac{\mu_L V}{\sigma_L \left(\dfrac{y}{\sigma_T} + \dfrac{w-y}{\sigma_L} \right) u_x}. \tag{90}$$

Integrating equation (90) we obtain

$$\frac{y(2\sigma_T w - y\sigma_T + y\sigma_L)}{2\sigma_T \sigma_L} = \frac{\mu_L V}{\sigma_L u_x} x + K, \tag{91}$$

where K comes from the constant of integration and is evaluated from the boundary condition. The interface between the trailing zone and the leading zone at the inlet is located at $y \approx 0$. Employing this boundary condition we obtain

$$y = -\frac{(\sigma_T w)}{(\sigma_L - \sigma_T)} + \sqrt{\left(\frac{\sigma_T w}{(\sigma_L - \sigma_T)} \right)^2 + \frac{2\sigma_T \mu_L V x}{(\sigma_L - \sigma_T) u_x}}. \tag{92}$$

Now we find the total resistance of the flow field, R, by considering the resistances of each segment in parallel:

$$R = \frac{1}{\int_{R(x=0)}^{R(x=l)} \frac{1}{dR}} = \frac{1}{\int_{R(x=0)}^{R(x=l)} \frac{hdx}{\left(\dfrac{y}{\sigma_T} + \dfrac{w-y}{\sigma_L} \right)}}. \tag{93}$$

After substituting in equation (92) and integrating we obtain

$$R = \frac{\dfrac{\left(\sigma_L - \sigma_T\right)2\sigma_T\mu_L V}{u_x}}{2\sigma_T\sigma_L h\left[\sqrt{\dfrac{\left(\sigma_L - \sigma_T\right)2\sigma_T\mu_L V}{u_x}l + \left(\sigma_T w\right)^2} - \sigma_T w \right]}. \tag{94}$$

For desalination to proceeded in the entire device, when $y = l, x = w$. Thus

$$\frac{V}{u_x} = \frac{w^2}{2\sigma_T\mu_L l}\left[\left(\sigma_L + \sigma_T\right)\right]. \tag{95}$$

Combining (94) and (95) we obtain

$$R = \frac{\left(\sigma_L + \sigma_T\right)\dfrac{w}{l}}{2\sigma_T\sigma_L h}. \tag{96}$$

The power consumed by the device is $P = V^2/R$. The energy per volume of processed fluid is given by the power per volumetric flow rate of the fluid. The volumetric flow rate is $Q_V = u_x wh$. Thus the ohmic energy per volume of processed fluid is

$$\frac{E_{ohm}}{V_{fluid}} = \frac{V^2}{Ru_x wh}, \tag{97}$$

which simplifies to

$$\frac{E_{ohm}}{V_{fluid}} = \frac{V\sigma_L}{\mu_L}. \tag{98}$$

To compare it to ohmic energy consumption derived in Section 2.6.3 in the main text (equation (12)) we expand (98) in terms of current density:

$$\frac{E_{ohm}}{V_{fluid}} = \frac{j}{\mu_L}\left(\frac{\sigma_L}{\sigma_T}d_T + d_L \right). \tag{99}$$

Next, to obtain a scaling, we approximate $d_T \approx d_L$ and obtain

$$\frac{E_{ohm}}{V_{fluid}} \approx \frac{jw}{\mu_L}\left(1 + \frac{\sigma_L}{\sigma_T} \right), \tag{100}$$

where w is the distance between the electrodes (analogous to H in equation (12) in the main text). Ohmic energy consumption in free flow and batch processes have similar scaling: ohmic energy consumption per volume of fluid processed scales proportional with current density, distance between the electrodes and the ratio of conductivities of the leading and trailing zone plus unity; and inversely with the mobility of the leading ion. The free flow process is analogous to many discrete batch wise channels moving in the direction of hydrodynamic flow while the interface inside the channels moves with electric field. Hence the overall energy consumption of both process scale similarly.

14.2 Pumping energy consumption in continuous free flow process

Here we estimate the pumping power requirement for a continuous free flow implementation of EPD. We estimate this based on the dimensions and typical flow rates of a commercially available continuous free flow electrophoresis system from Becton, Dickinson and Company (BD) (Planegg, Germany). This system has a separation chamber 10 cm wide (y-direction, see Figure SI 7), 50 cm long (x-direction), and 0.5 mm high and operates at a typical flow rate of 1 L/h[19]. The pressure drop across the chamber is equal to the energy per volume of fluid processed (i.e. the pumping energy). The pressure drop across a rectangular channel is given by:[20]

$$\Delta p = \frac{-3\mu Q_V l}{4\frac{h}{2}\left(\frac{w}{2}\right)^3 \left[1 - \frac{192w}{\pi^5 h} \sum_{i=1,3,5,...}^{\infty} \frac{\tanh\left(i\pi h/2w\right)}{i^5}\right]}, \tag{101}$$

where Q_V is the volumetric flow rate and μ is the dynamic viscosity of water. For the dimensions of this instrument and 1 L/h flow rate, we estimate that the pumping energy is approximately 1×10^{-8} Wh l^{-1}. This is approximately 8 orders of magnitude less than the minimum ohmic energy consumption and hence can be assumed negligible.

References

1. A. Persat, R. D. Chambers and J. G. Santiago, *Lab on a Chip*, 2009, **9**.
2. S. S. Bahga and J. G. Santiago, *Electrophoresis*, 2012, **in press**.
3. S. S. Bahga, M. Bercovici and J. G. Santiago, *Electrophoresis*, 2010, **31**, 910-919.
4. M. Bercovici, S. K. Lele and J. G. Santiago, *J. Chromatogr. A*, 2009, **1216**, 1008-1018.
5. J.Deman, *Analytical Chemistry*, 1970, **42**, 321-324.
6. F. M. Everaerts, J. L. Beckers and T. P. E. M. Verheggen, *Isotachophoresis: Theory, Instrumentation, and Applications*, Elsevier Scientific Publishing Co., Amsterdam, New York, 1976.
7. *Handbook of Chemistry & Physics*, CRC Press, Boca Raton, FL, 2011.
8. R. L. Dilworth, *Water Desalination*, Headquarters, Department of the Army, Washington D.C., USA, 1986.
9. J. P. Mericq, S. Laborie and C. Cabassud, *Water Res.*, 2010, **44**, 5260-5273.
10. R. O'Hayre, S.-W. Cha, W. Colella and F. B. Prinz, *Fuel Cell Fundamentals*, Wiley, 2005.
11. E. B. Anderson, E. J. Taylor, G. Wilemski and A. Gelb, *J. Power Sources*, 1994, **47**, 321-328.
12. J. Wang, N. V. Myung, M. Yun and H. G. Monbouquette, *J. Electroanal. Chem.*, 2005, **575**, 139-146.
13. R. K. Shervedani and A. Lasia, *J. Appl. Electrochem.*, 1999, **29**, 979-986.
14. L. L. Shreir, R. A. Jarman and G. T. Burstein, *Corrosion*, Elsevier, 1994.
15. L. J. J. Janssen and J. G. Hoogland, *Electrochim. Acta*, 1970, **15**, 941-951.
16. T. Kaneta, T. Ueda, K. Hata and I. Totaro, *J. Chromatogr. A*, 2006, **1106**, 52-55.
17. J. J. McKetta, *Encyclopedia of Chemical Processing and Design: Slurry Systems, Instrumentation to Solid-Liquid Separation*, M. Dekker, 1995.
18. Kašiǩa and V. Zdeněk Prusík, *J. Chromatogr. A*, 1987, **390**, 27-37.
19. BectonDickinson, *Operating Manual for BD™ Free Flow Electrophoresis System* Becton, Dickinson and Company, GmbH, Planegg, Germany, 2005.
20. F. M. White, *Viscous Fluid Flow*, McGraw-Hill, Inc., New York, USA, 1991.